

# MODEL INDEPENDENT DESCRIPTION OF FEL SHOT NOISE, AMPLIFICATION AND SATURATION USING GREEN'S FUNCTION

Yichao Jing\*, Vladimir N. Litvinenko, Yue Hao, Gang Wang  
 Brookhaven National Laboratory, Upton, NY 11973, USA

## Abstract

High-gain FEL is one of many electron-beam instabilities, which have a number of common features linking the shot noise, the amplification and the saturation. In this paper we present a new, model-independent description of the interplay between these effects and derive a simple formula determining the saturation and maximum attainable gain in such instabilities. Application of this model-independent formula to FELs is compared with FEL theory and simulations. We describe limitations resulting from these findings for FEL amplifiers used for seeded FELs and for Coherent electron Cooling.

## INTRODUCTION

FEL amplifiers can be used for a number of applications ranging from the HGHG [1], the coherent seed amplifying [2] or amplifier in Coherent electron Cooler [4]. Studies of gain and saturation in these FELs have captured wide interest and several criteria/estimations of saturation have been proposed [6, 7].

It is well known that e-beam instabilities, including those in FELs, can be described by a set of self-consistent Maxwell's and Vlasov equations. The Vlasov equation becomes nonlinear (which can cause the saturation of a FEL) when the density modulation becomes comparable with the initial beam density  $|\delta n| \sim n_0$ .

When  $|\delta n/n_0| \ll 1$  we can use linearized Vlasov equation, which then can be represented by Green's function. For compactness, we consider a one-directional instability (detailed derivation of 3D case is shown in [3]), where the response of the system on a perturbation can be described by one-dimensional Green's function,

$$n(\tau, z) = n_0 + \delta n + G_\tau(z - z_0), \quad (1)$$

where  $n_0$  is the initial electron beam density,  $\delta n = \delta(z - z_0)$  is a local perturbation at  $z = z_0$  and  $G_\tau(z - z_0)$  is the FEL's response on this perturbation at time  $\tau$ .

This 1D simplified model is usually true for a FEL, where diffraction makes transverse dependences smooth compared with the fast longitudinal oscillations. We also consider a response of the system to be much shorter compared with the electron bunch length, e.g. the e-beam density could be considered locally constant.

\* yjing@bnl.gov

## GREEN'S FUNCTION AND ITS SATURATION

As shown in Eq. 1, the electron distribution can be described by the initial density, local perturbation and FEL response – the Green's function. For a case of typical SASE FEL, the initial random distribution of electrons can be written as

$$n_0(0, z) = \sum_{i=1}^N \delta(z - z_i), \quad (2)$$

where  $N$  is the number of electrons in the bunch. If the system has external perturbations, e.g., when an ion bunch is co-propagating with the electron bunch as is for a Coherent electron Cooler (CeC) [5], the electron density, in the presence of modulation imprinted by ions with charge  $Z$  and effective density  $X \sim Z$ , becomes

$$n(\tau, z) = \sum_{i=1}^{N_e} \delta(z - z_i) + \sum_{i=1}^{N_e} G_\tau(z - z_i) + X \sum_{j=1}^{N_i} G_\tau(z - z_j). \quad (3)$$

For the modulation of interest, i.e., within a wavelet  $\{0, \lambda_0 = 2\pi/k_0\}$ , we can calculate bunching factor, corresponding to the relative local density modulation:

$$b(\tau) = \frac{\int_0^{\lambda_0} n(\tau, z) e^{ik_0 z} dz}{\int_0^{\lambda_0} n(\tau, z) dz}, \quad (4)$$

where  $M_e$  is the number of electrons in the wavelet  $\{0, \lambda_0\}$  and we define the gain of the modulation through the integral of the Green's function within the wavelet  $\{0, \lambda_0\}$  as

$$g(z_i) = \int_{-z_i}^{\lambda_0 - z_i} G_\tau(z) e^{ik_0 z} dz. \quad (5)$$

We can further define an effective correlation length  $N_c \lambda_0$ , which reads

$$\int_{-\infty}^{\infty} |g(z)|^2 dz = g_{max}^2 N_c \lambda_0 \quad (6)$$

Thus by assuming the FEL saturates at  $b(\tau) < 1$  or  $\langle |M_e b(\tau)|^2 \rangle < M_e$ , where  $M_e$  is the number of electrons in the wavelet  $\{0, \lambda_0\}$ , we arrive at

$$1 + g_{max}^2 N_c (1 + X^2 \frac{M_I}{M_e}) \leq M_e \quad (7)$$

which gives an estimate for the maximum attainable gain for an initial  $\delta$ -function like seed

$$g_{max} \leq \sqrt{\frac{M_e}{N_c (1 + X^2 \frac{M_I}{M_e})}}. \quad (8)$$

Table 1: e- Beam Parameters for FEL Simulation

Name	Infrared(PoP CeC)	Visible(eRHIC CeC)	VUV(LHC cooler)	Hard X-ray(LCLS)
Beam energy (MeV)	21.8	136	3812.3	13643.7
Beam current (peak,A)	100	10	30	3400
Normalized emittance ( $\mu m$ )	5	1	1	1.2
Fractional energy spread (dp/p)	$1 \times 10^{-3}$	$1.5 \times 10^{-5}$	$2.5 \times 10^{-5}$	$1.05 \times 10^{-4}$
Undulator period (cm)	4	3	10	3
Undulator strength $A_w(K_w/\sqrt{2})$	0.4	1	10	2.4756
$N_c$	35.8	102	70.6	14.5

In terms of peak current  $I_p$  and wavelength  $\lambda_0$  and in the absence of the ion bunch, we can rewrite Eq. 8 as

$$g_{max} \leq 144 \sqrt{\frac{I_p[A] \lambda_0[\mu m]}{N_c}}. \quad (9)$$

We arrive at a very neat formula for the maximum attainable gain where only the electron's peak current  $I_p$ , the FEL wavelength  $\lambda_0$  and coherent length (in terms of  $\lambda_0$ )  $N_c$  are involved. The result does not require the knowledge of the type of FEL or the properties of the electron beam (assuming it is suitable for FEL) and is fully applicable for 3D treatment. However, there is no analytical expression for  $N_c$  for an arbitrary 3D FEL.

## NUMERICAL ANALYSIS

We simulate a statistically representative set of initial shot noises with and without the seed (which has  $\delta$ -function like shape) in 3D FEL code Genesis 2.0 [8]. To extract the information of a  $\delta$ -function like seed with the existence of shot noises, we generate two bunches. The first bunch's initial distribution purely comes from random shot noises, i.e., from SASE signal. For the second bunch, we use quiet start to generate one seed slice with initial bunching factor at the level of interest, e.g.  $1e-4$ , then we superpose this slice on the middle of the first bunch. We propagate the two bunches (one with noise, one with noise and seed) through the FEL separately and obtain their bunching information (amplitude and phase) along the undulator. The bunching for the seed is simply the difference of these two results.

We have run simulation for a wide variety of scenarios in FEL spectrum ranging from infrared (CeC proof of principle), visible (eRHIC CeC), VUV (LHC cooler) to hard X-ray (LCLS). Detailed parameters are listed in Table. 1. Choosing the case of wavelength in visible(eRHIC CeC) range as an example, we calculate the averaged bunching over all 32 random shot noises for each slice within the electron bunch and show the maximum bunching amplitude in Fig. 1 as a function of the longitudinal position in the undulator. We calculate the difference between the two bunches, i.e., with and without initial seed, to extract the growth of the Green's function in the undulator and show it in Fig. 1 for comparison. Assuming there is no correlation between the shot noise and the initial seed, the two curves in Fig. 1 are representing different slices in the bunch and the slice #'s of both curves

change along the undulator due to slippage of a FEL. We notice that the response of the seed, after an initial delay, grows exponentially as the shot noise. During this initial delay, the bunching information, carried by the radiation, slides forward within the bunch and the maximum bunching amplitude of the response slightly decreases. The response saturates at the point where the shot noise saturates the entire bunch, i.e.,  $|b_{SASE}| \sim 1$ .

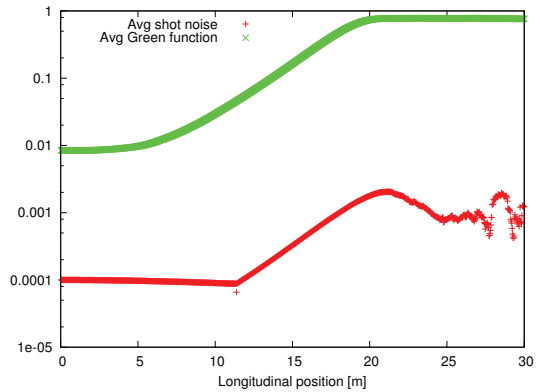
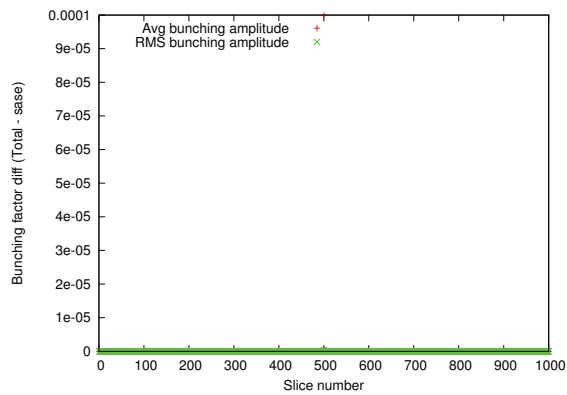


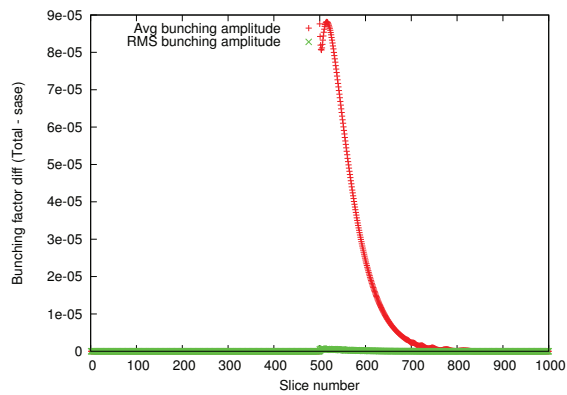
Figure 1: Plot of the FEL response's maximum bunching amplitude as a function of the longitudinal position in the undulator for noise+seed (green) and seed (red).

The entire process – the slippage, amplification and saturation of the FEL response – can be visualized by the evolution of the response's profile within the undulator, as is shown in Fig. 2 and Fig. 3. A seed is initially placed at the middle of the bunch with a bunching amplitude at  $1e-4$ . When the bunch propagates in the undulator, this seed slips forward and passes the bunch information to its "neighbouring" slices. The maximum bunch amplitude slightly decreases during this process. While the bunch continues its journey in the undulator, the head part of the bunch starts to overtake and grows exponentially. At the meantime, the variation of the response's bunch profile over different initial shot noises stays low. When the bunch approaches saturation, the variation of bunch profile starts to grow and overtakes its mean value. At such point, the response becomes completely noisy.

Content from this work may be used under the terms of the CC BY 3.0 licence (© 2014). Any distribution of this work must maintain attribution to the author(s), title of the work, publisher, and DOI.

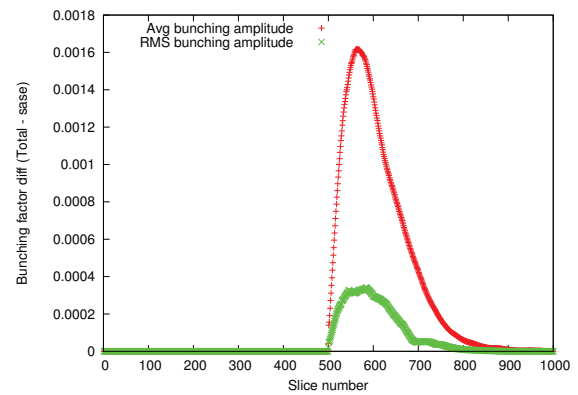


(a)

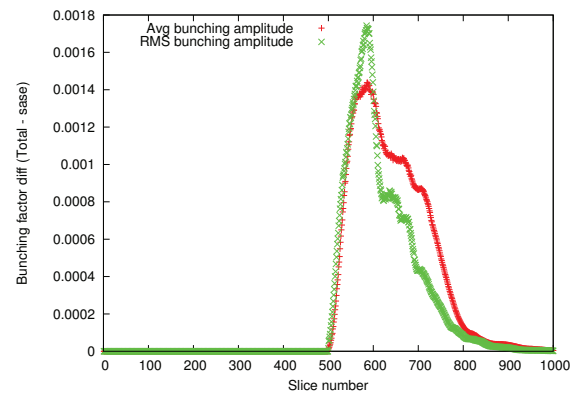


(b)

Figure 2: The bunching profile of the electron bunch in the undulator and its variation are plotted at (a)  $z=0.6$  m(start); (b)  $z=11.4$  m(the bunching factor of the head of the bunch starts to overtake and grows).



(a)



(b)

Figure 3: The bunching profile of the electron bunch in the undulator and its variation are plotted at (a)  $z=19.8$  m(close to saturation, the variation starts to grow); (b)  $z=22.0$  m(after saturation, the variation surpasses the bunching amplitude).

## COMPARISON AND DISCUSSION

The comparison of simulated maximum attainable gain in bunching factor and its theoretical estimation is listed in Table 2 with different scenarios that we study. The discrepancy between the simulated results and the theoretical estimations given by simple formula in Eq. 9 is generally within 20% except for the case of VUV where a 35% discrepancy is observed. Considering Eq. 9 is derived with 1D theory and without taking into account of many important 3D effects, the agreement is considered to be very good.

Table 2: FEL Gain of Theory and Simulation

Name	$g_{max,theory}$	$g_{max,simulated}$
Infrared	857.5	777
Visible	29.3	27
VUV	28.3	18.7
Hard X-ray	27	21.1

## ACKNOWLEDGMENTS

This work is supported by Brookhaven Science Associates, LLC under Contract No. DE-AC02-98CH10886 with the U.S. Department of Energy.

## REFERENCES

- [1] L.H.Yu, et al., Science 289, 932 (2000).
- [2] J Amann, et al., Nature Photonics 6, 693 (2012).
- [3] G. Wang, V.N. Litvinenko, C-AD note.
- [4] V.N.Litvinenko and Y.S.Derbenev, PRL 102, 114801 (2009).
- [5] V.N.Litvinenko, et al., Advances in coherent electron cooling, Proc. IPAC'14, MOPRO15.
- [6] E.L. Saldin, E.A. Schneidmiller, M.V. Yurkov, Physics Reports 260 (1995) 187-327.
- [7] S. Krinsky, AIP Conference Proceedings 648, 23 (2002).
- [8] S.Reiche, Genesis 2.0, manual on the website: <http://genesis.web.psi.ch/>
- [9] C. Gutt, et al., PRL 108, 024801 (2012).